Available online at www.sciencedirect.com

SCIENCE DIRECT®

International Journal of Multiphase Flow 32 (2006) 311–322

International Journal of Multiphase Flow

www.elsevier.com/locate/ijmulflow

Influence of gas injection on phase inversion in an oil–water flow through a vertical tube

M. Descamps [a,*], R.V.A. Oliemans [a], G. Ooms [a], R.F. Mudde [a], R. Kusters [b]

[a] *J.M. Burgerscentrum for Fluid Mechanics, Delft University of Technology, Kramers Laboratorium, Prins Bernhardlaan 6, 2628 BW Delft, The Netherlands*

[b] *Shell International Exploration and Production B.V., Kessler Park 1, 2288 GS, Rijswijk ZH, The Netherlands*

Received 12 June 2005; received in revised form 23 October 2005

Abstract

An experimental study has been made of the influence of gas injection on the phase inversion between oil and water flowing through a vertical tube. Particular attention was paid to the influence on the critical concentration of oil and water where phase inversion occurs and on the pressure drop increase over the tube during phase inversion. By using different types of gas injectors also the influence of the bubble size of the injected gas on the phase inversion was studied. It was found that gas injection does not significantly change the critical concentration, but the influence on the pressure drop is considerable. For mixture velocities larger than 1 m/s, the pressure drop over the tube increases with decreasing bubble size and at inversion can become even larger than the pressure drop during the flow of oil and water without gas injection.

Keywords: Three-phase flow; Phase inversion; Gas lift technique

1. Introduction

The gas lift technique is commonly used during oil production to reduce the pressure drop of a vertical well in order to enhance the oil production. It was shown by Guet et al. (2003), that the efficiency of the technique increases with decreasing bubble size of the gas injected into the flowing oil. However, not much is known about the efficiency of the gas lift technique for the case of a two-phase flow of oil and water through the production tube. There is evidence from the field that for certain conditions the gas lift technique is not working for a two-phase oil–water flow.

In a two-phase oil–water flow through a production tube phase inversion between oil and water can occur dependent on, for instance, the concentration of the two liquids. The speculation is, that the injection of gas can change the critical concentration of oil and water where phase inversion occurs and that the pressure drop increase during phase inversion can become larger. The phase inversion phenomenon has been investigated by

* Corresponding author. Tel.: +31 15 278 3210; fax: +31 15 278 2838.
E-mail address: m.descamps@tnw.tudelft.nl (M. Descamps).

0301-9322/$ - see front matter
doi:10.1016/j.ijmultiphaseflow.2005.10.006

various authors, experimentally (Ioannou et al., 2005; Bouchama et al., 2003) as well as numerically (Brauner and Ullmann, 2002; Chesters and Issa, 2004), but not much knowledge about the influence of gas injection on this phenomenon is available. In a recent study (Noui-Mehidi et al., 2004) an experimental investigation was made of phase inversion for the flow of oil and water in a mixing tank in the presence of small bubbles. The ambivalence range where both oil and water can be the continuous phase, was found to decrease due to the presence of the bubbles. However, to the best of our knowledge such an investigation has never been made for an oil–water flow through a vertical tube.

Therefore, we have made an experimental investigation of the influence of gas injection into an oil–water flow through a vertical tube. The results are reported in this publication. Particular attention is paid to the influence of gas injection on the critical concentration of oil and water where phase inversion occurs and on the pressure drop increase over the tube during phase inversion. By using different types of gas injectors the influence of the bubble size of the injected gas was also studied. Our experiments were carried out in the DONAU multiphase flow loop of Shell Exploration and Production Technology Applications and Research at Rijswijk in The Netherlands. As a reference we start with the results about phase inversion without gas injection. Thereafter the influence of gas injection will be presented.

2. Experiments

2.1. Description of the experimental facility

A picture of the DONAU multiphase-flow loop is given in Fig. 1. The test section can be inclined from 0° to 90° and was kept vertical for all the experiments described in this publication. The tube has a length of 15.5 m and the internal diameter is 82.8 mm. The pipe material is stainless steel AISI-316L, which is preferably wetted by the oil (hydrophobic wall). For flow visualization, a transparent perspex pipe section of length 1.15 m is used. The fluids used are salted water (brine) and oil (Vitrea 10) with properties listed in Table 1. Almost pure oil and water phases are pumped separately from a large coalescent-plate separator. The efficiency of the separation is validated by two Schlumberger Solartron 7835B densitometers, one for each phase at the outlet of the separator. The difference in density with values in Table 1 shows to be less than 2% during the tests. The fluids are then injected to a mixing section, and after a development section of 250 internal diameters they flow through the test section.

The following quantities are recorded:

- volumetric flow rates of oil and water by Micromotion CMD 50/100/200 Coriolis flow meters,
- pressure drop over a tube length of 10.35 m, by Rosemount 3051C differential, gauge and absolute pressure transducers,

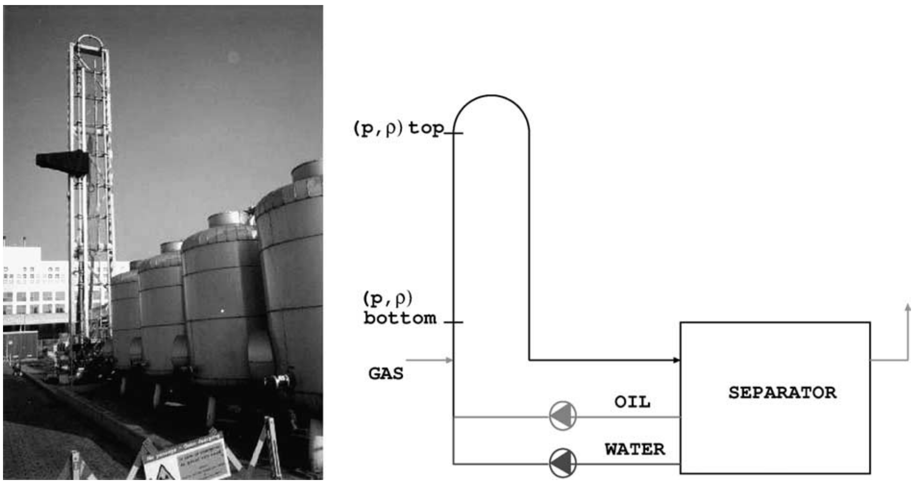

Fig. 1. Picture and sketch of the DONAU loop.

Table 1
Physical properties of liquids used

	Brine	Vitrea 10
Density at 40 °C (kg/m^3)	1060	830
Viscosity at 40 °C (mPa s)	0.85	7.5
Interfacial tensions at 25 °C (mN/m)		
Brine/air	50.7	
Oil/air	30.3	
Brine/oil	20.2	

- in situ liquid (oil and water) hold up, by Berthold LB 444 gamma ray densitometer,
- amplitude and phase of the conductivity of the liquid mixture via an impedance probe which consist of two coaxial electrodes placed perpendicular to the flow and connected to a lock-in phase analyser,
- video recording of the flow mixture using a Sony digital videorecorder DSR 20P.

The temperature is automatically controlled and regulated to 40 °C, within a range of 0.5 °C.

2.2. Measurement procedure

There are four sets of data. The first set consists of oil–water data without gas injection at different mixture velocities and different oil and water concentrations. Special attention is given to the critical concentration, where phase inversion takes place. In the second set gas injection occurs via a nozzle injector and attention is given to its influence on the critical concentration and on pressure drop over the tube. The third and fourth sets are similar to the second one, but measured with two different types of porous-material injectors in order to achieve smaller bubbles. There is a total of 234 measurement points. Each point requires 5 min recording at constant flow conditions, with a sampling frequency for the pressure transducers of 0.5 Hz.

3. Phase inversion in oil–water flow without gas injection

3.1. Flow pattern

During the experiments the mixture velocity is so large, that only dispersed flow occurs (oil drops in water or water drops in oil). This can be checked with the video recordings. In Fig. 2, the densities measured from the densitometer and calculated from water fraction are compared for different mixture velocity. All points are spread on a line that is just parallel to the unity line, which shows that the calibration of the densitometer is not perfect. Furthermore, it can be seen that no significant deviation of the density occurs when the mixture velocity changes from a low value to a higher value. Thus we conclude that the slip between the phases is negligible, and the homogeneous (no-slip) model can be applied, according to which the mixture density is a linear function of the oil (or water) fraction.

From the impedance probe we have information which liquid is the continuous phase and when phase inversion takes place.

The result is given in Fig. 3, which shows that phase inversion always takes place at a water concentration of about 30%, regardless the mixture velocity. This value is discussed in Section 5.

3.2. Pressure gradients

For fully developed (steady) dispersed flow the total pressure gradient is equal to the sum of the gravity pressure gradient and the frictional pressure gradient

$$\frac{\mathrm{d}P}{\mathrm{d}z} = \left(\frac{\mathrm{d}P}{\mathrm{d}z}\right)_{\mathrm{g}} + \left(\frac{\mathrm{d}P}{\mathrm{d}z}\right)_{\mathrm{f}}, \tag{1}$$

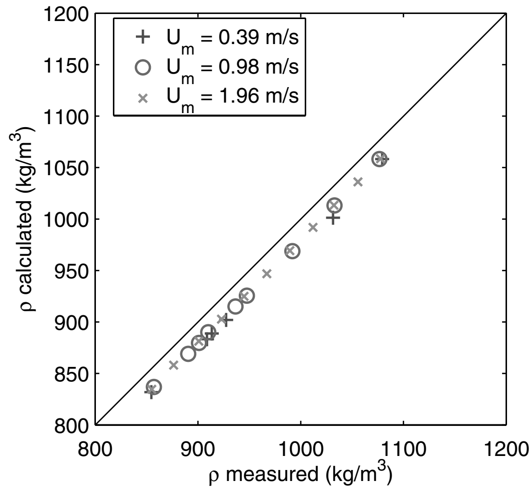

Fig. 2. Comparison between mixture density measured from γ-ray densitometer and calculated from water fraction.

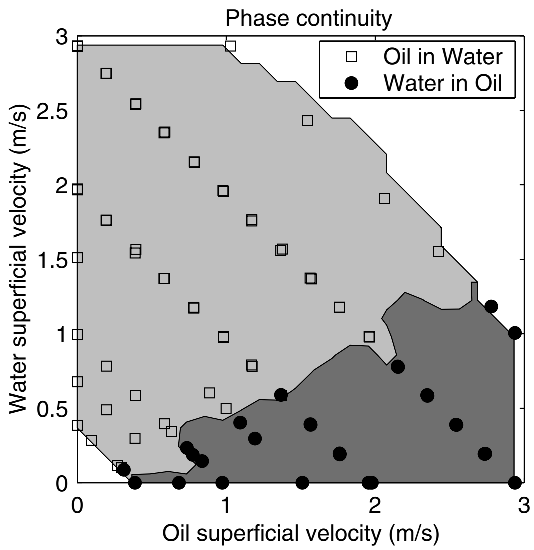

Fig. 3. Continuous-phase map.

in which P is the pressure and z the vertical coordinate. The gravity pressure gradient is given by

$$\left(\frac{\mathrm{d}P}{\mathrm{d}z}\right)_{\mathrm{g}} = \rho_m g \tag{2}$$

and the frictional pressure gradient by

$$\left(\frac{\mathrm{d}P}{\mathrm{d}z}\right)_{\mathrm{f}} = \frac{f_{\mathrm{m}}\rho_{\mathrm{m}}U_{\mathrm{m}}^2}{2D}, \tag{3}$$

where ρ_{m} is the mixture density, g the acceleration due to gravity, f_{m} the friction factor, U_{m} the mixture velocity and D the tube diameter. When we consider the liquid mixture as a homogeneous dispersion with an effective viscosity μ_{m}, f_{m} can be expressed as a function of the mixture Reynolds number $Re_{\mathrm{m}} = \rho_{\mathrm{m}}U_{\mathrm{m}}D/\mu_{\mathrm{m}}$ using an existing empirical correlation for a single-phase fluid. The following correlations are given in the literature (an overview of these correlations is found in Brauner (1998)):

(1) Blasius correlation for a tube with a smooth wall and for $2000 < Re_{\mathrm{m}} < 10^5$

$$f_{\mathrm{m}} = \frac{0.316}{Re_{\mathrm{m}}^{0.25}}. \tag{4}$$

(2) Colebrook correlation for a tube with rough walls

$$\frac{1}{\sqrt{f_{\mathrm{m}}}} = -2\log\left(\frac{k^*}{3.71} + \frac{2.52}{Re_{\mathrm{m}}\sqrt{f_{\mathrm{m}}}}\right) \tag{5}$$

with $k^* = k/D$ the non-dimensional wall roughness.

(3) Haaland correlation (see Haaland (1983))

$$f_{\mathrm{m}} = \left[-1.8\log\left(\frac{6.9}{Re_{\mathrm{m}}} + \left(\frac{k}{3.7D}\right)^{1.1}\right)\right]^{-2}. \tag{6}$$

3.2.1. Total pressure gradient

In Fig. 4 the total pressure gradient measured for six different mixture velocities is shown as function of the water fraction. For a mixture velocity below 1.5 m/s the pressure gradient exhibits a gravity dominated behavior with a linear increase from a pure-oil to a pure-water pressure gradient. The contribution due to the frictional pressure gradient is negligible. Above this velocity there is a noticeable peak in the pressure gradient due to the frictional component, in particular at the point of phase inversion (at a water fraction $\phi_{\mathrm{w}} \sim 0.3$). For the higher velocities experiments were carried out in both directions: from pure water to pure oil (squares) and vice versa (circles). This was done in order to observe a possible hysteresis effect described in publications about phase inversion (the so-called ambivalent range), also mentioned in the case of pipe flow (Ioannou et al., 2005). As can be seen this hysteresis effect does not occur during our experiments.

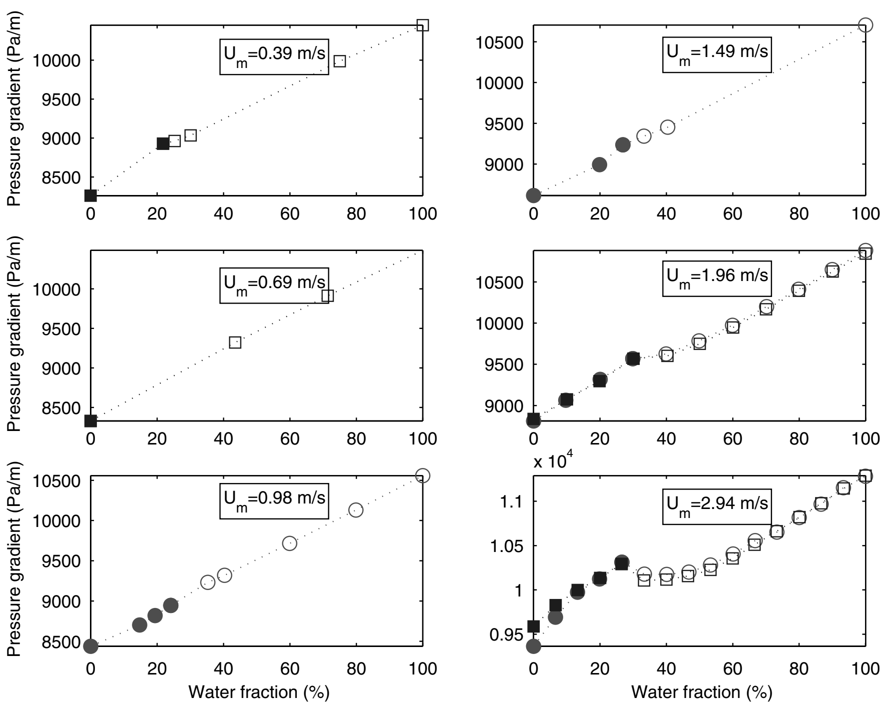

Fig. 4. Total pressure gradient for oil–water flow without gas injection. Squares: from water to oil, circles: from oil to water, open symbols: oil in water, closed symbols: water in oil.

3.2.2. Frictional pressure gradient

Using Eqs. (1) and (2) the frictional pressure gradient can be determined from the measured total pressure gradient. The resulting frictional pressure gradient as function of the water fraction for the six mixture velocities of Fig. 4 is shown in Fig. 5. The point of phase inversion is characterized by a peak in the frictional pressure gradient. At the high velocities this peak can be rather strong, due to a higher shear stress at the wall.

3.2.2.1. Measurement uncertainty. From the pressure measurement at bottom $\mathrm{d}P_{\mathrm{bot}}$ and at top $\mathrm{d}P_{\mathrm{top}}$ of the pipe, the frictional pressure drop is calculated as follows:

$$\left(\frac{\mathrm{d}P}{\mathrm{d}z}\right)_{\mathrm{f}} = \frac{\mathrm{d}P_{\mathrm{bot}} - \mathrm{d}P_{\mathrm{top}}}{L} - \rho_{\mathrm{m}} g. \tag{7}$$

In terms of experimental uncertainty, this can be written as

$$\Delta\left(\frac{\mathrm{d}P}{\mathrm{d}z}\right)_{\mathrm{f}} = \sqrt{\frac{\varepsilon_P^2}{L^2}(\mathrm{d}P_{\mathrm{bot}}^2 + \mathrm{d}P_{\mathrm{top}}^2) + \varepsilon_\rho^2 \rho_{\mathrm{m}}^2 g^2}. \tag{8}$$

The uncertainty on the frictional pressure gradient is a combination of the relative uncertainty on the pressure measurements ε_P, which is less than 0.2% and the experimental uncertainty on the density ε_ρ which is much higher (around 1%). For lower velocities $U_{\mathrm{m}} < 1.5$ m/s, where friction does not play a significant role in the pressure gradient, the error bars become larger than the variations themselves (Fig. 5), so it is not relevant to draw conclusions on these plots.

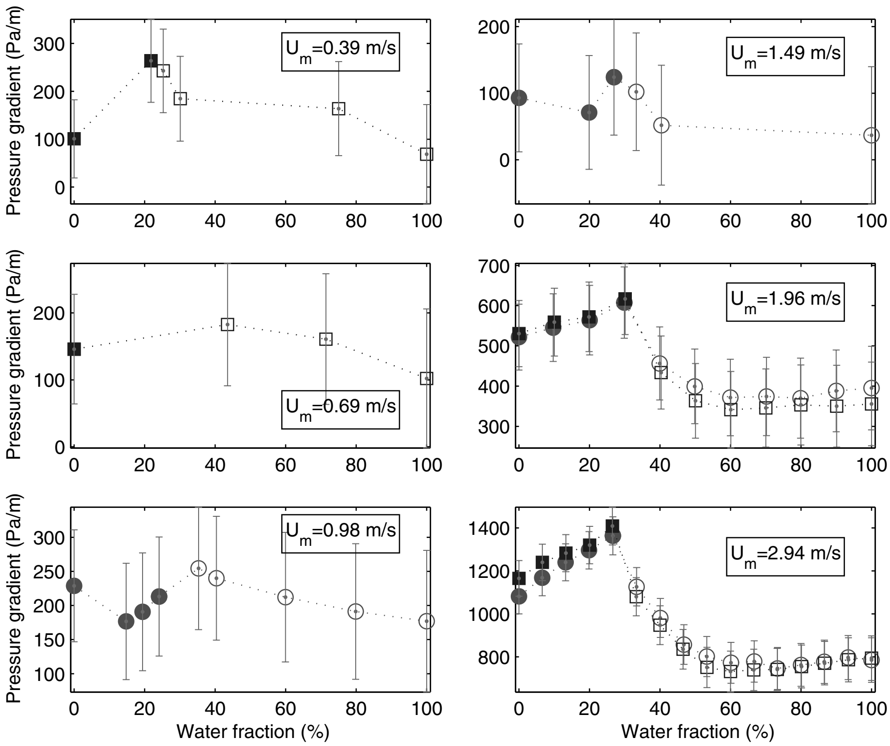

Fig. 5. Frictional pressure gradient for oil–water flow without gas injection. Squares: from water to oil, circles: from oil to water, open symbols: oil in water, closed symbols: water in oil.

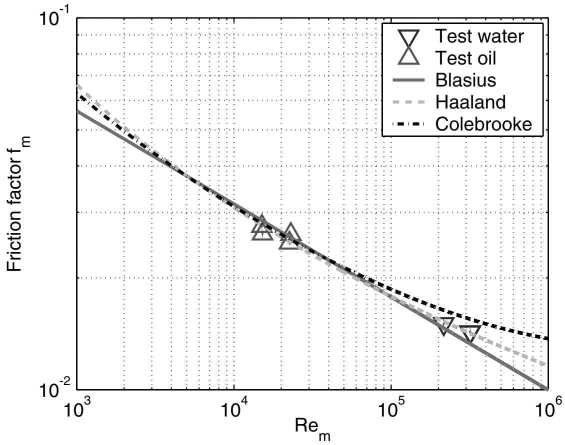

Fig. 6. Friction factor as function of Re_m: comparison between single-phase experiments points and correlations taken from literature.

3.2.3. Single-phase flow friction factor

We have compared the friction factor as calculated from Eqs. (4)–(6) with the friction factor as determined from our single-phase (pure oil or pure water) flow experiments. The results are shown in Fig. 6, where the friction factor is plotted as function of Re_m. Only flow rates corresponding to $U_m > 1.5$ m/s have been used, as the results for lower velocities are not reliable (as observed in Section 3.2.2). The agreement between predictions made with the correlations and our experimental data is good for all three correlations, although the Haaland correlation gives a slightly better agreement than the other two.

3.2.4. Effective viscosity of the mixture

When we assume that the single-phase flow correlations for the friction factor also hold for a homogeneous two-phase flow, we can (by using one of these correlations) determine the effective mixture viscosity from our experiments. We have applied the Blasius correlation for this purpose. The calculated effective viscosity as function of the water fraction (ϕ_w) is given in the left part of Fig. 7 for three values of the mixture velocity. Re_m is shown as function of the water fraction in the right part of Fig. 7 for the same three velocities. The peak amplitude of the effective viscosity at phase inversion increases with mixture velocity. For $U_m = 2.94$ m/s the effective viscosity at phase inversion is two times the pure oil viscosity. The increase in mixture viscosity at phase inversion implies a reduction in the Reynolds number at phase inversion, but the flow remained always turbulent during our experiments.

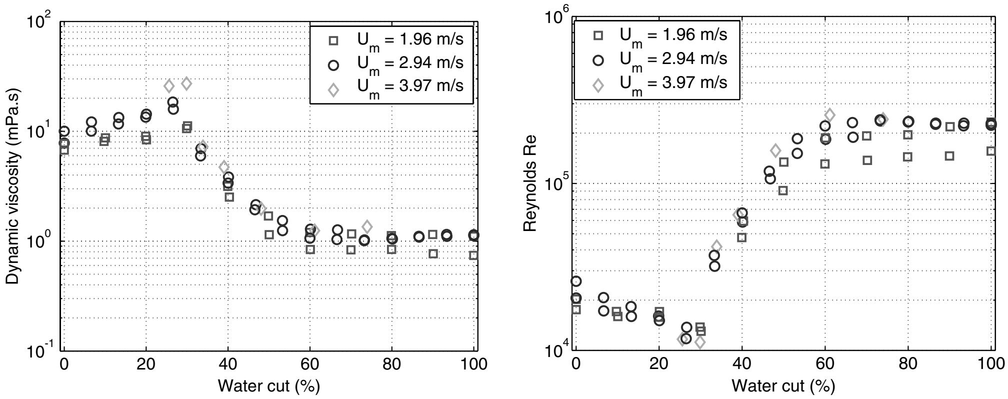

Fig. 7. Effective mixture viscosity and Reynolds number as function of water fraction.

Three parts are visible in Fig. 7:

- $\phi_w < 0.3$: oil is continuous phase, effective viscosity grows exponentially (with growth rate increasing with mixture velocity), Re_m is smaller than Re_{oil}.
- $0.3 < \phi_w < 0.6$: water is continuous phase, oil concentration is high, effective viscosity decreases exponentially (independent of mixture velocity), Re_m increases.
- $\phi_w > 0.6$: water is continuous phase, oil concentration is low, effective viscosity is constant, $Re_m = Re_{water}$.

4. Effect of gas injection on phase inversion

As mentioned the aim of this study is to investigate the influence of gas (air) injection on phase inversion in a dispersed oil–water flow through a vertical tube. Particular attention is paid to the influence of the bubble size of the injected gas on the critical concentration where phase inversion takes place and on the pressure drop over the tube during phase inversion. For this purpose three types of injectors were used (see Fig. 8):

- the nozzle injector, which is a small pipe with an internal diameter of 4 mm located in the middle of the test tube generating large (about 10 mm) bubbles;
- the conical porous injector, which consists of a cone of porous material placed over the outlet of the nozzle injector generating smaller (about 3 mm) bubbles;
- the circular porous injector, which is a ring of porous material inserted inside the tube against the tube wall generating also 3 mm bubbles.

Using video recording two flow regimes were identified during the experiments: slug flow and dispersed flow. At high mixture velocities ($U_m > 1$ m/s) the flow pattern is always dispersed flow (gas bubbles in a water-in-oil emulsion or gas bubbles in an oil-in-water emulsion). At lower velocities ($U_m < 1$ m/s) the flow pattern is slug flow. In this study no in situ measurements of bubble size has been performed.

4.1. Pressure gradient

During the experiments it became clear, that the bubble size has almost no effect on the critical concentration where phase inversion takes place ($\phi_w \sim 0.3$). However its influence on the pressure drop over the tube during phase inversion is considerable. For the sake of simplicity we will discuss the experimental results for low and high mixture velocities separately.

4.1.1. Low mixture velocity ($U_m < 1$ m/s)

The results of these experiments are given in Fig. 9, in which the total pressure gradient is plotted as function of the water fraction for four different conditions. For a mixture velocity of $U_m = 0.39$ m/s there are two values for the gas-volume fraction (GVF = 2.56% and 9.52%); for a mixture velocity of $U_m = 0.98$ m/s there are also two values for the gas-volume fraction (GVF = 2.05% and 7.28%). In each of the four figures the results are given for the three different types of injector; for comparison also the result for oil–water flow with-

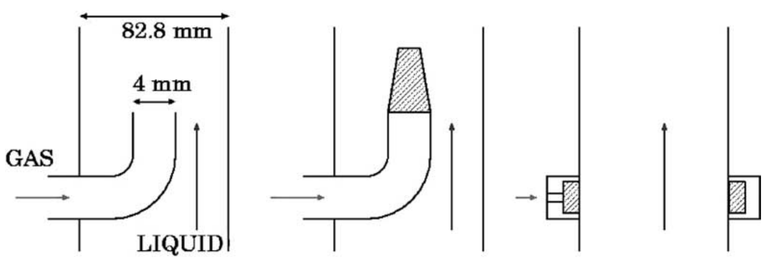

Fig. 8. Three types of gas injectors, from left to right: nozzle injector, conical porous injector, circular porous injector.

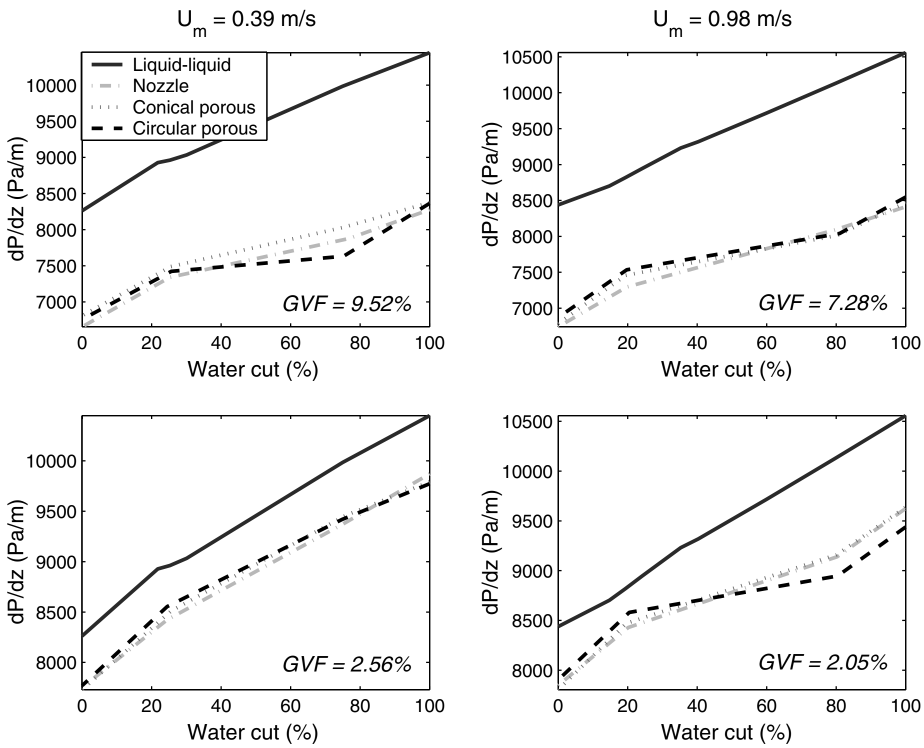

Fig. 9. Total pressure gradient as function of water fraction for an oil–water flow with gas injection for several values of the mixture velocity and the gas volume fraction and for different types of injector (for $U_m < 1$ m/s).

out gas injection is shown. As mentioned the gas injection does not influence the critical concentration ($\phi_w \sim 0.3$) where phase inversion occurs, but it has a significant influence on the pressure drop over the tube. As in the case of a single liquid, gas injection decreases the pressure drop (also during the point of phase inversion). The pressure drop decreases with increasing gas injection. It decreases more at large values of the water fraction than at smaller values. The difference in influence for the different type of injectors is rather insignificant. The circular porous injector are a bit more effective than the other two injectors in the water-continuous region ($\phi_w > 0.3$); but in the oil-continuous region (($\phi_w < 0.3$)) the other two are slightly more effective. The conical porous injector has about the same influence as the nozzle injector.

4.1.2. High mixture velocity

The results for the high mixture velocities are shown in Figs. 10 and 11. Fig. 10 gives the pressure gradient as function of the water concentration for three values of the gas volume fraction. Fig. 11 shows the pressure gradient as function of the water fraction for the three types of injectors. For comparison also the result for the oil–water flow without gas injection is provided. Phase inversion always takes place at a water fraction of about $\phi_w \sim 0.3$. It is evident from the figures that the pressure drop peak during phase inversion is much stronger enhanced at high mixture velocities than at low velocities. The magnitude of the peak is not very dependent on the gas volume fraction. As can be seen in Fig. 10 at a low value of the gas volume fraction the peak can even cross the pressure-gradient line for the case of oil–water flow without gas injection for values of the water fraction around the phase inversion point. So for such conditions gas injection has a negative effect on the pressure drop over the tube; the gas lift technique does not work for such conditions. As shown in 11 the peak is strongly dependent on the type of gas injector. The circular porous injector causes the highest peak. This is very surprising as for a single-liquid flow it was shown, that the pressure drop over the tube decreases with decreasing bubble size. However for gas injection in a two-phase flow the pressure drop increases with decreasing bubble size, in particular at the point of phase inversion.

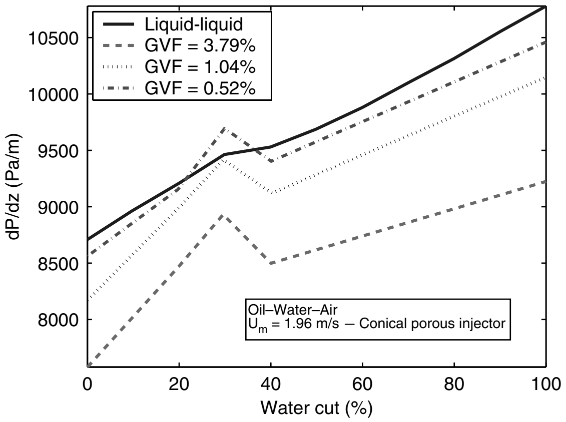

Fig. 10. Total pressure gradient as function of water fraction for an oil–water flow with gas injection for three values of the gas volume fraction (for $U_m > 1$ m/s).

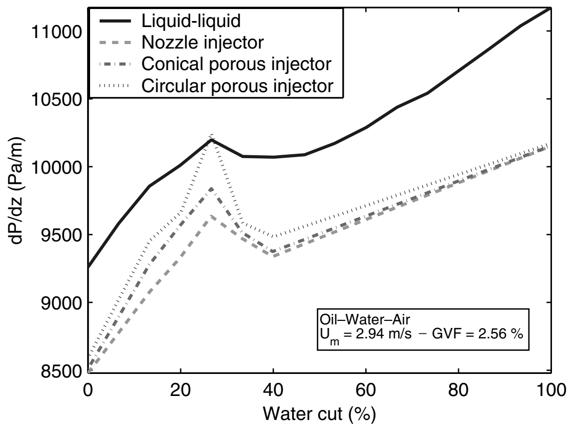

Fig. 11. Total pressure gradient as function of water fraction for an oil–water flow with gas injection for three types of gas injectors (for $U_m > 1$ m/s).

5. Discussion

Various mechanisms for the occurrence of phase inversion are found in literature, including packing concentration of spheres (Nunez et al., 1996) or the development of multiple emulsions (Chesters and Issa, 2004). The 30% inversion point is compared with a few published models or correlations in Table 2, where μ, $\tilde{\rho}$ and $\tilde{v}$ are, respectively, the dynamic viscosity, the density ratio between oil and water and the kinematic viscosity ratio between oil and water. As can be seen, all the values are very close but the critical fraction of water at inversion point is best predicted by the model of Brauner and Ullmann (2002), which involves the minimization of the total energy of the system.

In the following we mention a few points that can perhaps explain the interesting results of our phase inversion experiments with gas injection. We will investigate these points in our future (experimental) research.

- The different behavior at low mixture velocities and high mixture velocities can be attributed to differences in the characteristic size of drops and bubbles. At low mixture velocities the drop and bubble sizes are mainly determined by the entry conditions (similar to bubbly flow in gas–liquid systems) rather than by the turbulence intensity, as in the case of high mixture velocities.

Table 2
Prediction of inversion point

Authors	Water cut at inversion point	Application
Yeh et al. (1964)	$1\Big/\left(1+\left(\frac{\mu_0}{\mu_\mathrm{W}}\right)^{0.5}\right)$	0.4
Arirachakaran et al. (1984)	$0.5-0.1108\log\left(\frac{\mu_0}{\mu_\mathrm{W}}\right)$	0.25
Brauner and Ullmann (2002)	$1-\tilde{\rho}\tilde{v}^{0.4}/(1+\tilde{\rho}\tilde{v}^{0.4})$	0.33

- The changes observed by varying the water cut at low mixture velocities are a result of gradual flow pattern transitions between water dominated to oil dominated flow patterns, through an intermediate churn flow zone. (This is similar to the sequence of flow pattern transitions in vertical gas–liquid flows. With increasing gas velocity the flow pattern changes from bubbly flow to annular flow.) This gradual flow pattern transition is not to be confused with the phase inversion that takes place at high mixture velocities.
- The bulk viscosity of the mixture is not important for the pressure drop which is balanced by shear stresses at the wall. Therefore the mixture viscosity at the wall is important. So it is relevant to determine what is preferentially on the wall; gas, oil or water. In particular it is important to find out, where the gas is. It can be expected that it is always in or on the oil, irrespective whether the oil is continuous or dispersed (gas hates water).

6. Conclusion

An experimental study has been made of gas injection in oil–water flow through a vertical tube. Special attention was given to the influence of gas injection on the phase inversion process between oil and water. As a reference the flow of oil and water without gas injection was investigated first.

From the experiments without gas injection it can be concluded, that the effective viscosity increases considerably during phase inversion leading to a pressure peak over the tube at the phase inversion point. The data show that the growth of the effective viscosity increases with increasing mixture velocity. This may be due to the change in turbulence at higher mixture velocities. More detailed experiments are needed to confirm this assumption. The hysteresis effect during phase inversion as found in other studies was not found during our experiments. The point of phase inversion was always close to a water fraction of $\phi_\mathrm{w} = 0.3$, independent on the direction of change in water fraction during the experiments (from oil to water or from water to oil).

From the experiments with gas injection it was found, that gas injection does not influence the critical oil or water concentration where phase inversion takes place. However gas injection strongly enhances the pressure-drop peak at phase inversion. The peak can even cross the (pressure-gradient-versus-water-fraction) line for the case of oil–water flow without gas injection for values of the water fraction around the phase inversion point. So for such conditions gas injection has a negative effect on the pressure drop over the tube and the gas lift technique does not work anymore. With decreasing bubble size this effect becomes even stronger. This is very surprising as for gas injection in a single-liquid flow it was shown, that the pressure drop over the tube decreases with decreasing bubble size. This important result cannot be explained by us at the moment. Obviously the bubbles play an important role during phase inversion, but it is not clear which role that is. In our future work we will make a detailed study of this phenomenon.

Acknowledgements

Financial support was provided by Shell Exploration and Production. The author is grateful to Hans den Boer for his support and continuous interest. Special thanks to Arno van den Handel and Danny Kromjongh for their valuable contribution and patience in running the experimental setup.

References

Arirachakaran, S., Oglesby, K., Malinowsky, M., Shoham, O., Brill, J., 1984. An analysis of oil/water flow phenomena in horizontal pipes. In: SPE Prof. Prod. Operating Symp. Oklahoma, US.

Bouchama, F., van Aken, G., Autin, A., Koper, G., 2003. On the mechanism of catastrophic phase inversion in emulsions. Colloids Surf. A: Physicochem. Eng. Aspects 231 (1–3), 11–17.

Brauner, N., 1998. Liquid–Liquid two-phase flow. HEDU—Heat Exchanger Design Update, pp. 1–40 (Chapter 2.3.5).

Brauner, N., Ullmann, A., 2002. Modeling of phase inversion phenomenon in two-phase pipe flows. Int. J. Multiphase Flow 28, 1177–1204.

Chesters, A., Issa, R., 2004. A framework for the modelling of phase inversion in liquid–liquid systems. In: 5th International Conference on Multiphase Flow, ICMF'04, Yokohama, Japan.

Guet, S., Ooms, G., Oliemans, R., Mudde, R., 2003. Bubble injector effect on the gas lift efficiency. AICHE J. 49 (9), 2242–2252.

Haaland, S., 1983. Simple and explicit formulas for the friction factor in turbulent pipe-flow. J. Fluids Eng. Trans. ASME 105 (1), 89–90.

Ioannou, K., Nydal, O., Angeli, P., 2005. Phase inversion in dispersed liquid–liquid flows. Exp. Therm. Fluid Sci. 29, 331–339.

Noui-Mehidi, M., Wu, J., Zhu, Y., 2004. A few new findings on phase inversion in a liquid/liquid system. AICHE J. 50, 3281–3283.

Nunez, G., Briceno, M., Mata, C., Rivas, H., Joseph, D., 1996. Flow characteristics of concentrated emulsions of very viscous oil in water. J. Rheol. 40 (3), 405–423.

Yeh, G., Haynie, F., Moses, R., 1964. Phase–volume relationship at the point of phase inversion in liquid dispersions. AICHE J. 10, 260–265.